Final Report to PICCC

"Climate Change Impacts on Critical Ecosystems in Hawai'i and US Pacific Islands Territories"

Addendum to the Report from March 2013

PI: Oliver Elison Timm, Intl. Pac. Res. Ctr., Univ. Hawai'i-Mānoa, 1680 East-West Rd, Honolulu, Hi, 96822, USA

Co-PIs: Thomas W. Giambelluca, Dept. Geog., Univ. Hawai'i-Mānoa, 2424 Maile Way, Honolulu, HI, 96822, USA;
Henry F. Diaz, CIRES, Univ. Colorado - Boulder, 216 UCB, Boulder, CO 80309, USA

Funding Period: October 2010 - December 2012

Date of Report: January 23th, 2014

Submitted by: Dr. Oliver Elison Timm

Executive Summary

This addendum to the final report presents several important results that were missing in the final report from March 2013 (FR201303). The main purpose of this report is to summarize the downscaling results for the dry season, which was not done in FR201303. We also extend the report by presenting projected rainfall change maps for the wet and dry season at the end of the 21st century. Feedback from PICCC pointed out that the previous report was missing a comprehensive discussion of the confidence ranges and sources of uncertainty about the results, and a statement on the extent to which the regional features on the maps are trustworthy. In response, we now include a discussion about how the magnitude of the projected changes should be interpreted, and why generally much larger drying trends are projected than in a previously published scenario, which was developed with a different set of station data, large-scale climate predictors and different climate change model scenarios. We note that some of the work presented here is not exclusively derived from the PICCC project, but is also an integral part of a current PICSC project. This represents a continued effort to improve the statistical downscaling methods, and spatial mapping of the projected rainfall changes.

The addendum is structured as follows:

Results from the wet and dry season are presented in detail. We added additional summarizing statistics that characterize the trends for the individual islands and that can be better compared with direct outputs from IPCC reports and models. We also summarize confidence and uncertainty measures of the projected rainfall change patterns and amplitudes.

In another section, we report on the available products and their data formats. In the Appendix we included a short explanation of sources of uncertainty in the statistical downscaling that can assist users of the data products in the interpretation of the downscaled rainfall changes. However, we do not presume to impose our own interpretation upon the reader/user of the products in regards of their particular applications of our results.

1. Accomplishments:

Interpolated rainfall anomalies expressed in percentages of the 1978-2007 climatological mean (Rainfall Atlas of Hawai‘i, 2011) for the wet season November-April and dry seasons (May-October) are shown in the figures below. Maps were generated for Big Island (BI) Maui Nui (MA), O‘ahu (OA), Kaua‘i (KA) using ordinary kriging. Maps are presented for two Representative Concentration Pathways (RCP4.5, and RCP8.5) for a mid-21st century interval (average for the years 2041-2071) and a late 21st century period (2071-2100) from the CMIP5 ensemble median output.

The following adjective terms are used to express confidence (or uncertainty) in the projections; such a definition is only loosely tied to statistical-mathematical measures of confidence (uncertainty):

Very low: region with no stations or no stations with statistically robust cross-validation.
Low: few stations and/or stations with inconsistent trends but all stations with some skill.
Medium: good station coverage with consistent cross-validation correlation values and consistent trends.
High: high cross validation skill and values for the estimated changes remain in a moderate physically consistent range.
Very high: highest calibration and highest cross validation skill, no ambiguous surrounding stations and within a well-defined ‘climate zone’.

We will frequently use the terms ‘*relative anomalies*’ or ‘*percentage anomalies*’ to describe the estimated rainfall changes. The former expresses these changes relative to the 1978-2007 mean climatological values as reported in the Rainfall Atlas of Hawai‘i (Giambelluca et al., 2013). For example a value of -20% relative anomaly in a region with 200 inches of mean seasonal rainfall would indicate a projected 40-inch decrease. Rainfall anomalies in units of inches will be explicitly indicated as such.

The term *amplitude* or *magnitude* is used to describe the value of the changes irrespective of the sign. For example a -50% change or +50% change are both considered changes with large amplitudes or magnitudes compared with -5% or +5% changes. The use of these terms does not necessarily reflect the amplitude of the changes in the rainfall amounts in inches.

The presented maps describe climatological changes in the seasonal rainfall averaged over ~30 years. 30-yr intervals are standard time-averaging intervals recommended by the WMO and widely accepted in climate change research as an averaging interval. Year-to-year and decadal fluctuations will continue in future and we do not report here if and how this climate variability will change. Thus, individual seasons will always look different than the 30-yr averages presented here.

Lastly, the results are the median results from 32 CMIP5 state-of-the-art climate models. We have chosen these models without guidance from model performance tests or model evaluation metrics. Nor have these models been selected or rejected to promote a certain type of large-scale climate change projection pattern. The selection was simply based on the data availability at the time of our statistical downscaling analysis.

We present here the median result from these models such that at each grid location half of the downscaled models project lower values, and half of the model project higher values. The median values are more robust against outliers than the multi-model ensemble mean values.

1.1 Wet and Dry Season Projections

The various projection maps are shown in Figures 1-8. We first consider changes on a statewide basis followed by discussion of individual islands patterns that indicate somewhat different responses from the overall patterns, for the two projection periods and the two RCP scenarios.

For the wet season, the overall pattern projected for the Hawaiian Islands can be described as "*The dry gets dryer and the wet remains wet or gets wetter*". The relative anomalies are highly correlated with mean annual rainfall, with dry areas getting much drier and wet areas changing less in relative terms, some drying some getting wetter (Fig. 1). This pattern is most evident over Maui Nui and Hawaiʻi Island during the wet season (Figs. 21, 25). Categorized by the present-day average rainfall amounts, we see a clearly organized change in the sign of the projected rainfall anomalies. On Kauaʻi and Oʻahu the largest amplitude in the relative changes are seen in the lowest rainbands and lowest amplitudes in the relative changes of the wettest rainfall bands (Figs. 13, 17). The pattern for the RCP8.5 simulations (Fig. 2) is similar to the RCP4.5, but with higher amplitude, showing the greater effects of the higher emissions and radiative forcing implicit in this scenario. For the late 21st century RCP4.5 ensemble median changes (Fig. 3), the pattern is similar to the mid-century RCP4.5, but with higher amplitude in the areas experiencing drying. This shows that the dry areas will continue to get drier throughout the century with the magnitude of change dependent on the strength of the radiative forcing, whereas relatively little change will occur in the wetter areas in the latter part of the century. Figure 4 illustrates projected wet season changes for the high emissions scenario. The pattern is similar to the RCP4.5, but with much higher amplitude in the areas experiencing drying. This shows that the dry areas will experience extreme reductions in rainfall by the end of the century under a business-as-usual scenario (RCP8.5). However, we see in the summary statistics for the different rain band categories that these high-amplitude signals expressed in relative units with respect to the present-day climatology can be compensated by small changes in the rain bands with high rainfall amounts (compare Figs. 21 and 22 for Maui Nui and Figs. 25 and 26 for Big Island.)

Figure 5 illustrates changes for the dry season, mid-21st century RCP4.5 scenario. Compared with the wet season results (Figures 1-4), the downscaled precipitation change pattern appears more diversified across the Islands. On Kauaʻi, where, according to our statistical analysis, the influence of the large-scale circulation is not as effective as during the wet season (and our downscaling model is not very robust over the observed period 1978-2007, see Figures 10 and 12), the statistical downscaling results in small rainfall change anomalies (see also Figs. 15,16, 29). On the other hand, the middle islands experience the most drying, which is especially widespread on the islands of Maui Nui. The Oʻahu pattern is very similar to the wet season pattern, with pronounced drying in the drier areas, and relatively small changes in the wetter areas (Figs, 5-8,19). However, for the total freshwater balance of Oʻahu the changes over the Koʻolau mountains in the wettest rainbands become very important (Figs. 19, 20, 29). Most of Hawaiʻi Island shows drying. Figure 6 shows the dry season, mid-21st century RCP8.5 scenario. The pattern is similar to the RCP4.5, but with much higher amplitude, showing the greater effects of the higher emissions implicit in this scenario. Severe rainfall reductions are seen throughout the islands of Maui Nui. The corresponding late 21st century RCP4.5 map (Fig. 7) shows a pattern similar to the RCP4.5, but with higher amplitude in the areas experiencing drying. This shows that the dry areas will continue to get drier throughout the century under a middle-of-the-road scenario and may experience extreme reductions in dry season rainfall (Fig. 8). Regarding the overall freshwater balance the changes in the wettest rain bands contribute the largest to the overall rainfall amount reduction over Maui Nui (Figs. 23, 24, 29) and Hawaiʻi Island (Figs. 27, 28, 29).

1.2 Discussion of the confidence in the rainfall change projections

In general, the confidence in the emerging rainfall anomaly pattern appears consistent with the recent trend in regional rainfall changes, in particular in the dry areas. In the past, however, yearly to decadal variability in the rainfall anomalies was dominated by rainfall anomalies having the same sign in the wet and dry regions of the individual island groups. El Niño years, for example, cause statewide dry anomalies (even on the wet sides we find negative anomalies).

Our statistical downscaling results project the emergence of opposing trends during the wet season. These contrasting trends seen in the regional pattern are a consequence of the projected large-scale circulation changes over the North Pacific in the future climate, and not necessarily related to the typical modern ENSO pattern. In particular, Maui, the Big Island and Oʻahu show increases in wet areas. These regions are found along the east-facing sides and over the Koʻolau mountains on Oʻahu, on the east facing slopes of Haleakalā and on West Maui. On Big Island the eastern side of from Hilo along the Hāmākua Coast up to North Kohala we observe positive trend over the eastern slopes, including the Puna district. The lower-elevations between Mauna Kea and Mauna Low, this positive anomaly stretches into the central parts of Big Island. Whereas we have reasons to give medium to high confidence into the positive anomaly structures in these regions that see most of their rainfall coming from trade-wind induced precipitation, the demarcation line between positive and negative anomalies is of lower confidence. Interpolation methods in areas with sparse observations such as over central parts of Big Island contribute to the uncertainty.

It is noteworthy that on Kauaʻi, we do observe only negative anomalies in the pattern emerging in the future scenarios. We attribute this to the fact that over Kauaʻi changes the in Kona low weather and frontal rainfall competes with the trade-wind induced rainfall anomalies, and the rainfall deficit resulting from fewer or less intense extra-tropical disturbances in the future dominates over any potential increase in rainfall amounts during the trade-winds.

In the sequence of projected changes from the mid to late 21st century, we see that the dry anomalies grow in amplitude much more strongly than do the wet anomalies. We find: the greater the severity of the future warming scenario, the larger the amplitude of the negative rainfall anomalies. The locations with the maximum drying trends, however, remain the same. The most pronounced drying trends measured relative to the present-day rainfall rates are found on west Kauaʻi from Hanapepe/Waimea to the Nā Pali coast. On Oʻahu, the Waiʻanae coast, Waipahu, Pearl City are centers of the drying trends; Wailuku and Makawao are the areas on Maui with the largest amounts in relative rainfall decrease; and on Big Island, areas along the Kohala coast from Kawaihae to Kailua-Kona have the largest amplitudes in the relative negative trends. A secondary center is located around South Point.

When interpreting future trends derived from downscaling, our confidence decreases the further we project into the future (see Appendix). Large relative precipitation anomalies of more than -60% can be found on Kauaʻi, Oʻahu and Maui in the RCP8.5 scenarios (Fig. 4). These numbers are associated with large numerical uncertainties from the statistical model. Furthermore, non-linear effects that are not included in the linear regression model will play a larger role the further the projected changes deviate from the present-day conditions. Finally, it has been shown that the seasonal mean rainfall in these dry regions is controlled by a few heavy rain days in the season, and as such the statistical downscaling method is trying to 'emulate' changes in such heavy rain events. All these factors contribute to a reduced confidence in the more extreme late 21st century scenarios and the confidence in the amplitude of the changes is low. However, the confidence in location of the drying pattern is at medium levels. With a careful monitoring of the upcoming trend pattern, we will, therefore, have an opportunity to identify regions where drying trends can be expected to continue into the next decades.

The dry season signals and pattern are generally less certain and the overall confidence is low. Very low confidence should be attributed to the projected changes on Kauaʻi. Given that the projected amplitudes are small and remain small in the 21st century, we have limited skills to infer even the sign of the trends (Fig. 5-8).

On Oʻahu, the dry season trend pattern shows the largest relative changes towards dryer conditions from the Waiʻanae coast inwards to Waipio and the Ewa Plain. In the more severe RCP8.5 scenario and for the end of century projection, west Oʻahu and the southern coast to Makapuʻu show strong drying tendencies. Even over the eastern section and the Ko‘olau range the downscaling results indicate a -10 to -20% change in rainfall.

Over Maui, the statistical downscaling projects a widespread decrease in the dry seasonal rainfall. As amplitude increases with the severity in the RCP scenario and with time, less regional features are projected over Maui. This is consequence of the low downscaling skill in many parts of Maui Nui. Local rainfall patterns and large-scale circulation are not strongly linked. Future circulation changes do not provide enough information for locally enhanced or reduced rainfall trends over Maui. A general decrease in rainfall during the summer season may be a consequence of the stronger warming in the middle atmosphere, which stabilizes the atmosphere, and thermally-induced convection over the interior of the island may be suppressed in a warming climate. Future research will be needed to raise our confidence in the drying trends projected for Maui and currently the confidence is very low in the amplitude and low in the ‘featureless’ pattern.

Similarly, the drying trends over Big Island are not well understood physically. However, the statistical downscaling exhibits a higher confidence for the projected changes in the eastern part of the island. The central band with largest negative trend amplitudes extends from the extreme dry western coastal regions in North Kohala to the wet regions in Hilo on the east coast. Based on interpretation of our statistical downscaling, it is currently not possible to identify a demarcation line where trade-wind induced rainfall changes are replaced by changes in other mechanisms, most likely land-sea-breeze controlled precipitation. Therefore we estimate the location and amplitude of the drying trends with low confidence in the east and very low confidence in the west.

As final note: In the statistical downscaling of Maui, we included Moloka‘i, Lāna‘i and Kaho‘olawe. The regional features on Moloka‘i appear to follow the wet-dry pattern during the wet season. Lāna‘i has its own set of stations and cross validation skills (Figures 9-12), which suggest similar skills as on the eastern sides of Maui. As such, the confidence is high for the sign of the changes and medium for the wet season amplitudes. The dry season must be considered with medium to low confidence.

Kaho‘olawe on the other hand, the available stations did not qualify for the statistical downscaling (sample problem). Hence all results shown here are extrapolations from nearby stations from West Maui and Lāna‘i. Thus the confidence in the resulting changes in medium to low regarding the sign, but we have very low confidence in the amplitude of such changes.

3. Concluding Remarks

The summary of the statistical downscaling results shows that regionally different rainfall trends are likely to enhance the contrast between the wet and dry rainfall regions on the Islands of Hawai'i. This pattern (*'the dry gets dryer, and the wet gets wetter'*) is a feature of the wet season and associated with circulation changes unrelated to the typical El Nino - Southern Oscillation pattern. The confidence in this pattern conservatively estimated is moderate (based on the statistical methods and the physical understanding of the future circulation changes). However, similar patterns are seen in the independently derived rainfall anomalies by Dr. Kevin Hamilton and Dr. Chunxi Zhang (regional climate model results from the WRF model at the IPRC, University Hawaii, pers. communication). The dry season pattern and amplitudes of the projected changes have low confidence. Overall our new results project strong drying trends in the dry areas of Hawaii, Maui Nui and Oahu. By the late 21st century the projected changes in the circulation pattern become very large and the climate change signal amplitudes much stronger. With the current methods applied this makes our downscaling more sensitive to the underlying assumptions of linearity and, secondly, the stationarity assumption (what we observed and learned from the past is applicable to the future climate). Yet, we see that the emerging rainfall anomaly patterns itself are robust against the choice of the specific scenario and time horizon.

Appendix

A Review of the statistical downscaling method

Our statistical downscaling method is similar to the methods widely used in atmospheric sciences and climate change research. This section is intended to give the user of the downscaling results/products help to understand our confidence and uncertainty discussion.

At the heart of our downscaling method is the well-known linear regression model. Linear regression is useful to approximate a connection between two variables, without necessarily having knowledge of the causal relationships. A popular example is the relationship between body weight and height of the person. Yet, we know from our own experience that this relationship is not very accurate and does not work in every single case. Further, one could question whether a linear statistical relationship derived using data from the past can be expected to give reliable projections of future events. What is important, however, is to choose reasonable variables that are known to represent a physical process link between the predictand (e.g., the weight of a person) and the predictor (e.g., the height). We also can easily infer from common experience that other factors such as age, gender could play an important role in determining the weight of a person.

In our case, the predictand is the seasonal rainfall at sites on the Hawaiian Islands; the predictors are found in the patterns of large-scale circulation over the Pacific. We choose from a huge pool of possible predictors a subset of large-scale climate factors based on our prior knowledge. Improvements in accuracy of the downscaling can, therefore, be expected if future research results improve our theoretical understanding of the climate dynamics and rain-producing mechanisms. The regression models may, therefore, experience significant changes in future. Yet, it is unlikely that the most prominent statistical relationships exploited here do not represent a real physical connection, based on the empirical evidence that corroborate our statistical regression model. Consider the above weight-height relationship example. The general positive correlation (taller people on average weigh more) is physically robust and the opposite relation is highly unlikely. In our downscaling results, we are also having high confidence in the qualitative results between the large-scale circulation anomalies (such as El Niño events) causing dryer than normal conditions; lower confidence is projected for the amplitude estimates (either dimensional or relative changes in the rainfall) caused by the changes in the large-scale circulation.

Linear regression models are most accurate near the center of our empirical samples. The center of the observed predictand data is tightly connected to the mean of the predictor data. All regression lines are uncertain due to imperfect knowledge about the true relationships. As shown in Figure A1, small uncertainties in the fitted regression line's slope are amplified towards the extremes of the sample space. In our case the uncertainties of the projections increase as the projected changes in rainfall increase.

Finally, we point out that, for obvious reasons, linear regression cannot reduce or eliminate uncertainty originating from climate change scenarios. If the predictor is loosely defined, then the same will be true of the predictand. In the weight-height regression example, uncertainty about the height of a new person will propagate through the regression line and add uncertainty to the estimate of the person's weight. But it is also noteworthy that linear regression does not add additional uncertainty to the predictand, it just puts uncertainty into a quantifiable perspective what we lack in the fundamental understanding of the physical causative processes.

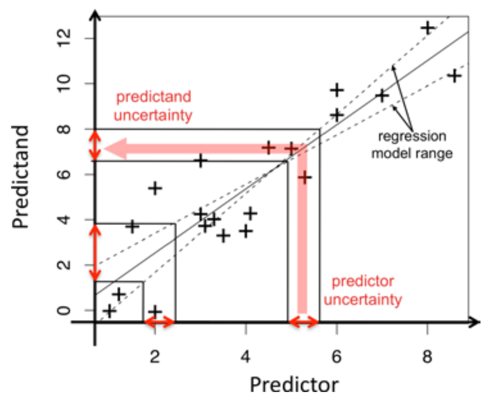

Figure A1: Illustration of the different sources of uncertainty in a linear regression model. Uncertainty in the predictor variable is propagated onto the predictand. In addition, uncertainty about the slope of the regression line (the regression coefficient) will lead to larger uncertainty in the extremes of the predictor range.

B. Figures

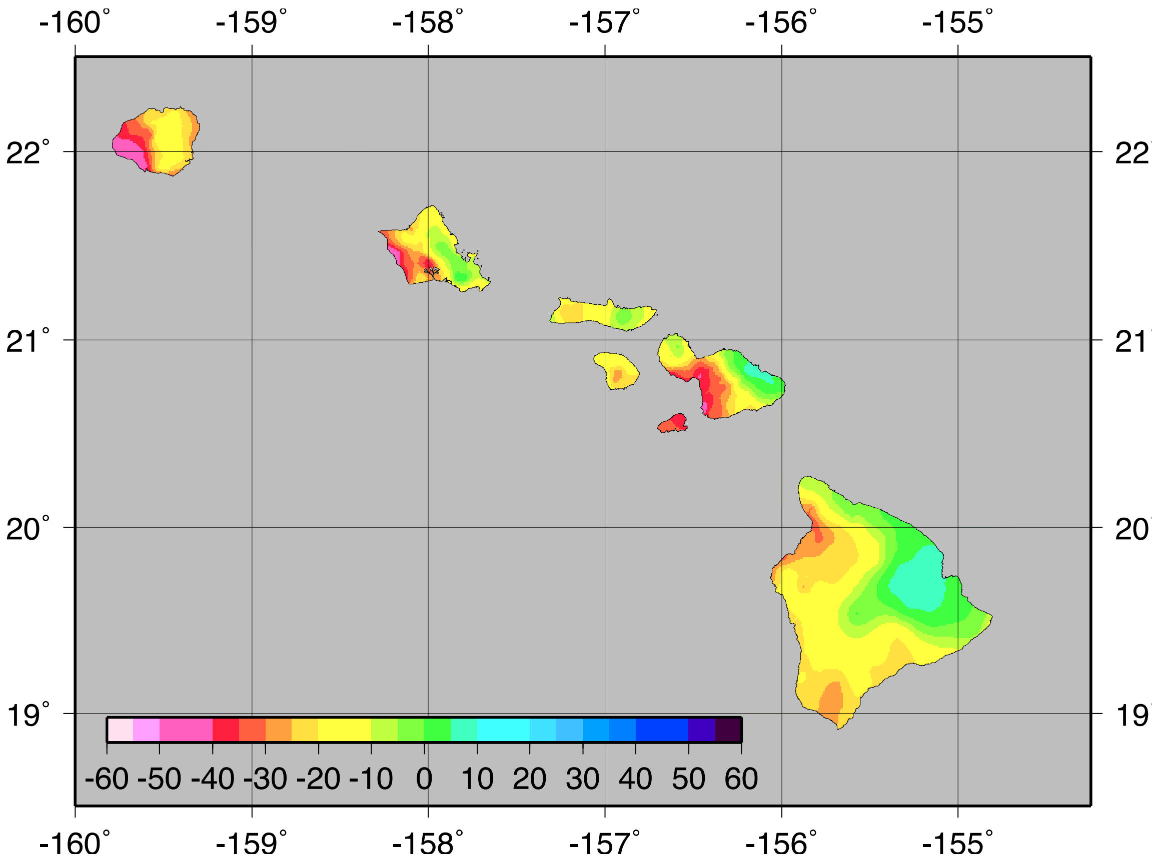

Figure 1: Interpolated rainfall anomalies expressed in percentages of the 1978-2007 climatological mean (Rainfall Atlas of Hawai'i, 2011) for the wet season November-April. Maps were generated for Big Island (BI) Maui Nui (MA), O'ahu (OA), Kaua'i (KA) using ordinary kriging.Shown is the mid-21st century scenario from the CMIP5 RCP4.5 ensemble median (average for the years 2041-2071). Units are given in percent.

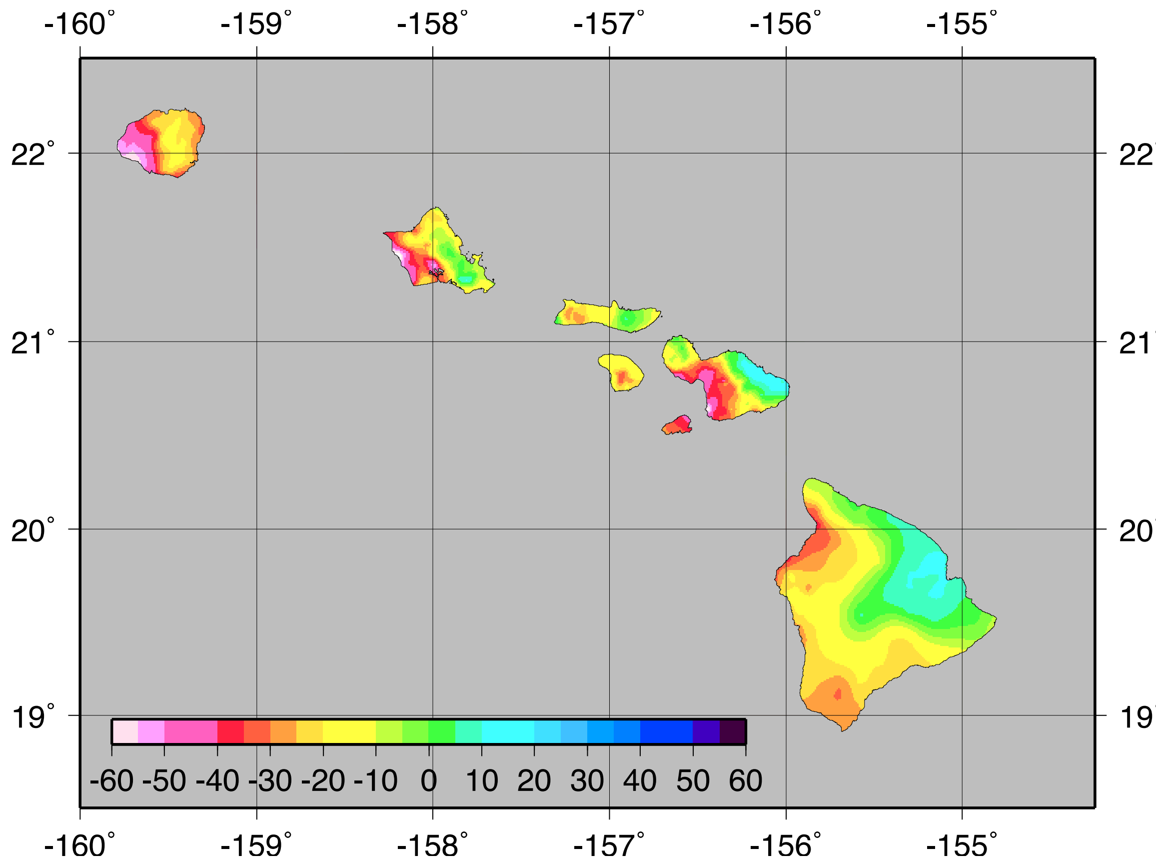

Figure 2: Same as Figure 1, but for the wet season in the RCP 8.5 ensemble median scenario (2041-2071 average).

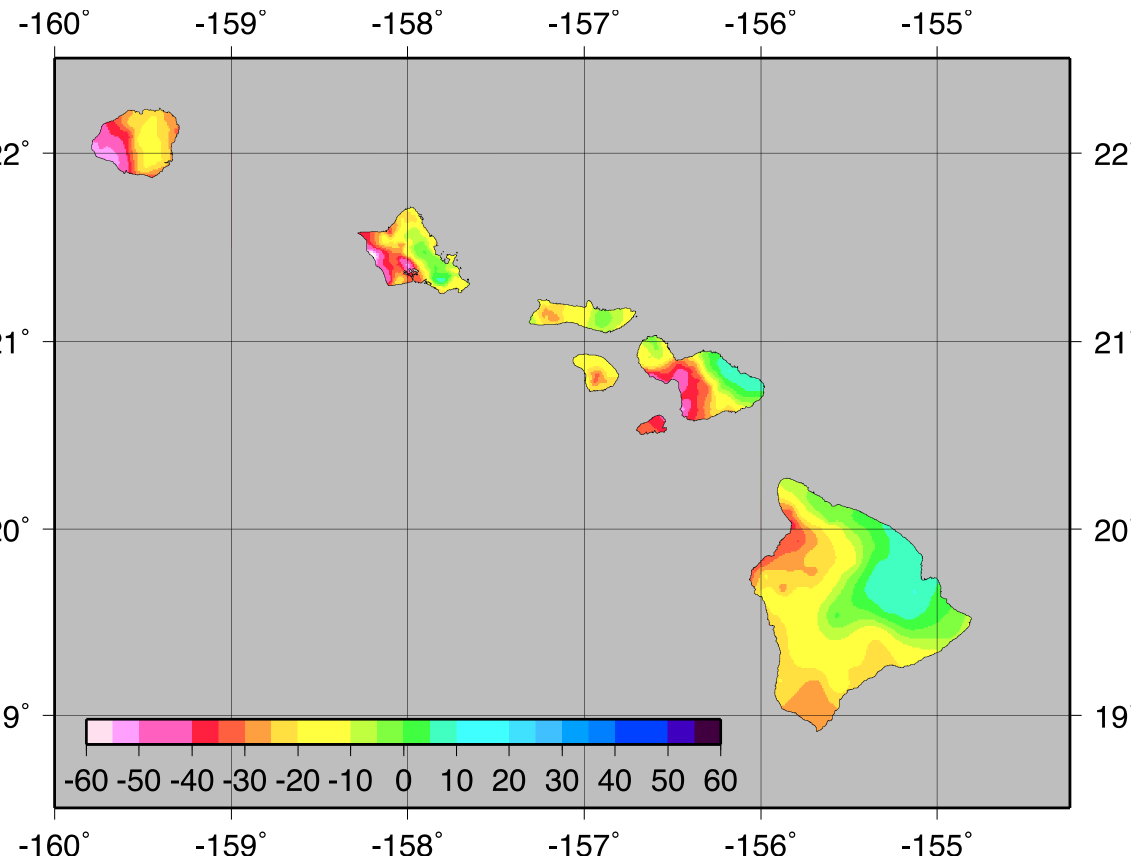

Figure 3: Same as Figure 1, but for the wet season in the RCP 4.5 ensemble median scenario late 21st century (2071-2099 average).

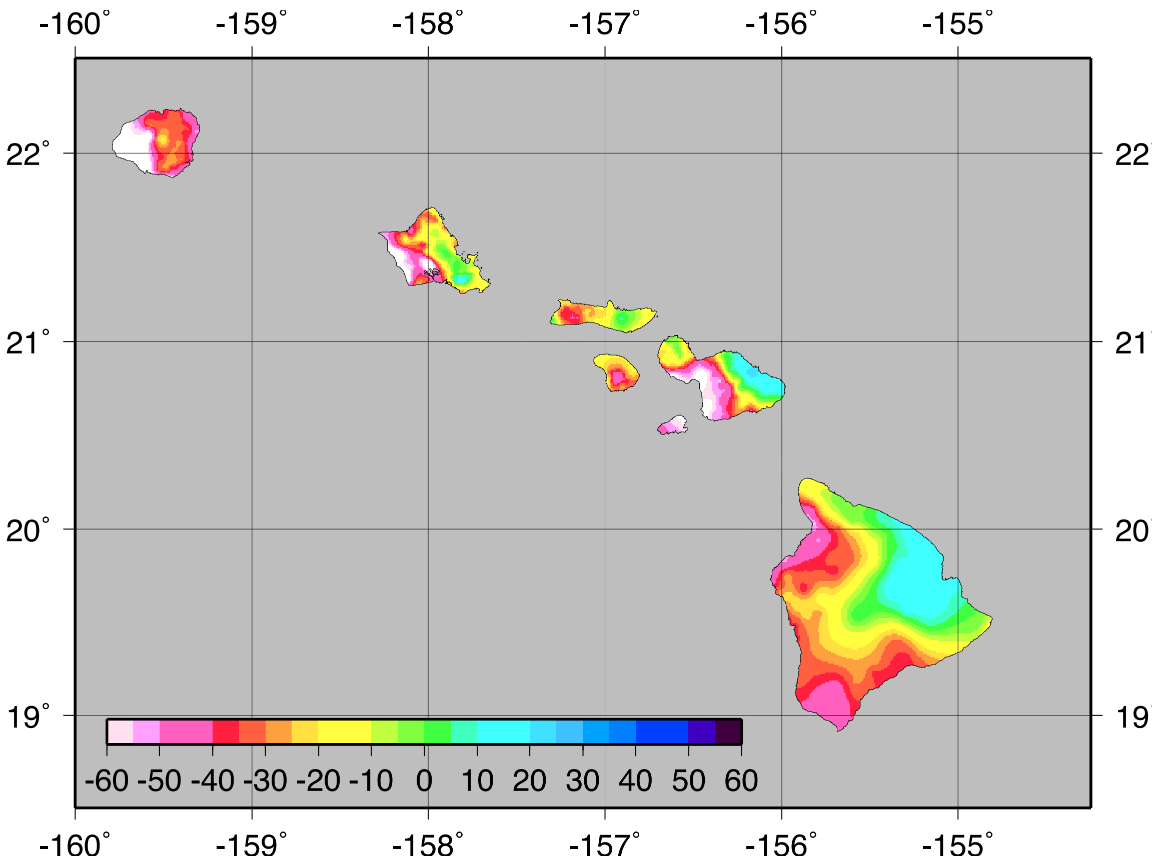

Figure 4: Same as in Figure 3, but for the wet season in the CMIP5 RCP8.5 ensemble median scenario late 21st century (2071-2099 average). Note that the linear regression model estimates very large (negative) anomalies for leeward parts of Kaua'i, O'ahu, Maui. In general, our confidence in the magnitude of the estimated extreme anomalies are low for the estimates obtained with our linear statistical downscaling for the ensemble median in the more severe RCP 8.5 scenario by end of the century. However, qualitatively the patterns of the rainfall changes remain stable (see Figure 1-4).

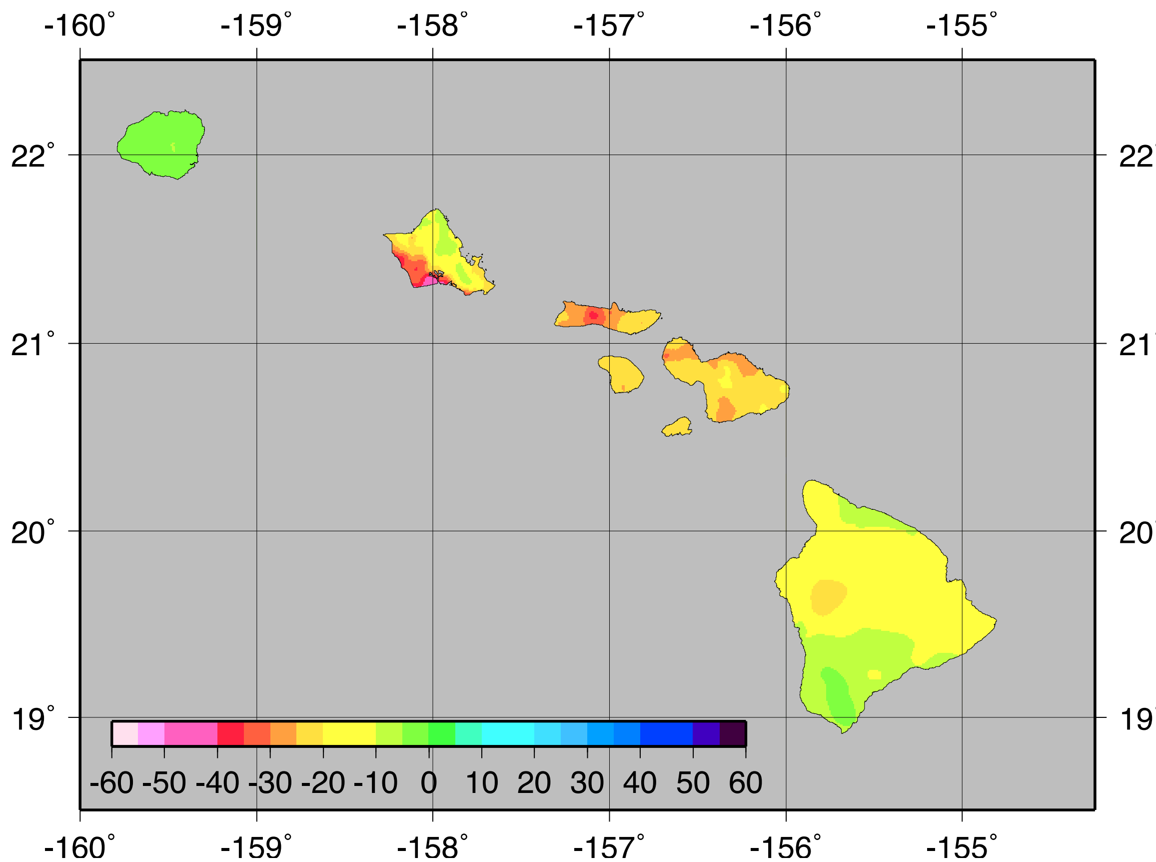

Figure 5: Interpolated rainfall anomalies expressed in percentages of the 1978-2007 climatological mean (Rainfall Atlas of Hawai'i, 2011) for the dry season April-October. Maps were generated for Big Island (BI) Maui Nui (MA), O'ahu (OA), Kaua'i (KA) using ordinary kriging. Shown is the mid-21st century scenario from the CMIP5 RCP4.5 ensemble median (average for the years 2041-2071). Units are given in percent.

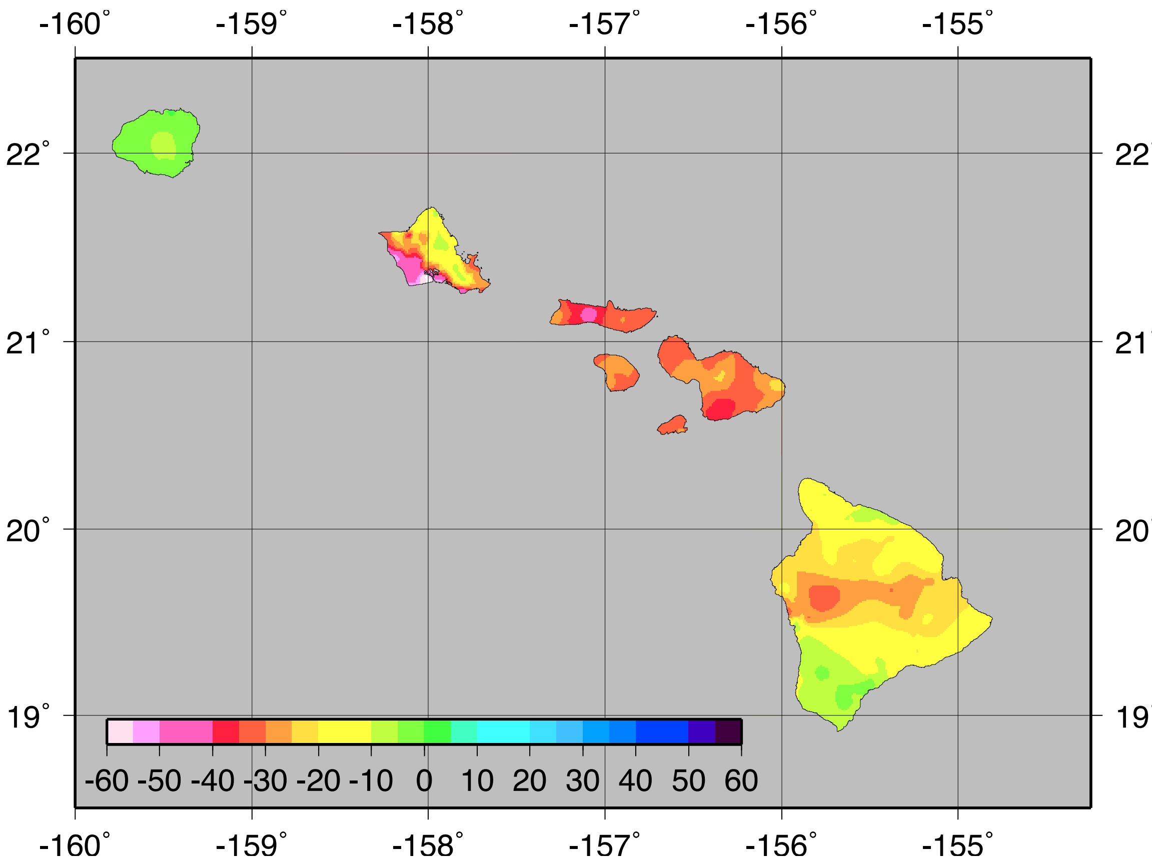

Figure 6: Same as Figure 5, but for the dry season in the RCP 8.5 ensemble median scenario (2041-2071 average).

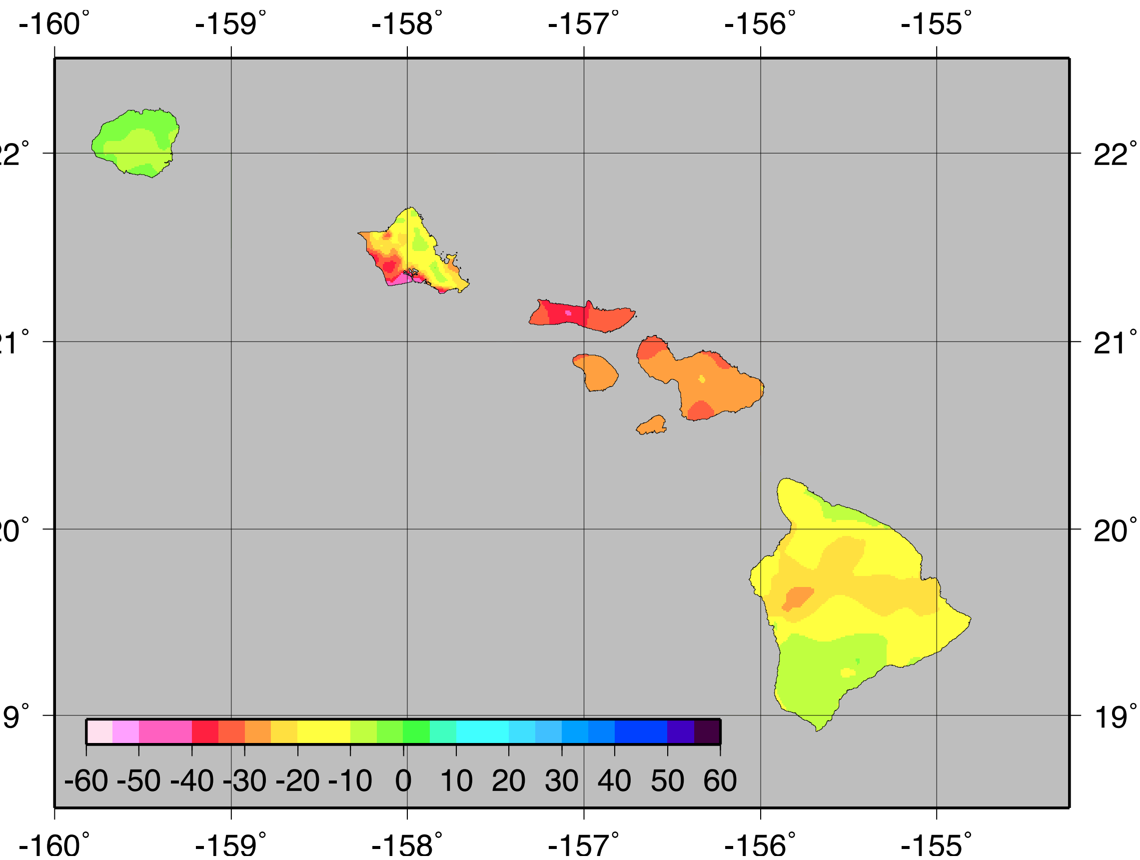

Figure 7: Same as Figure 1, but for the dry season in the RCP 4.5 ensemble median scenario late 21st century (2071-2099 average).

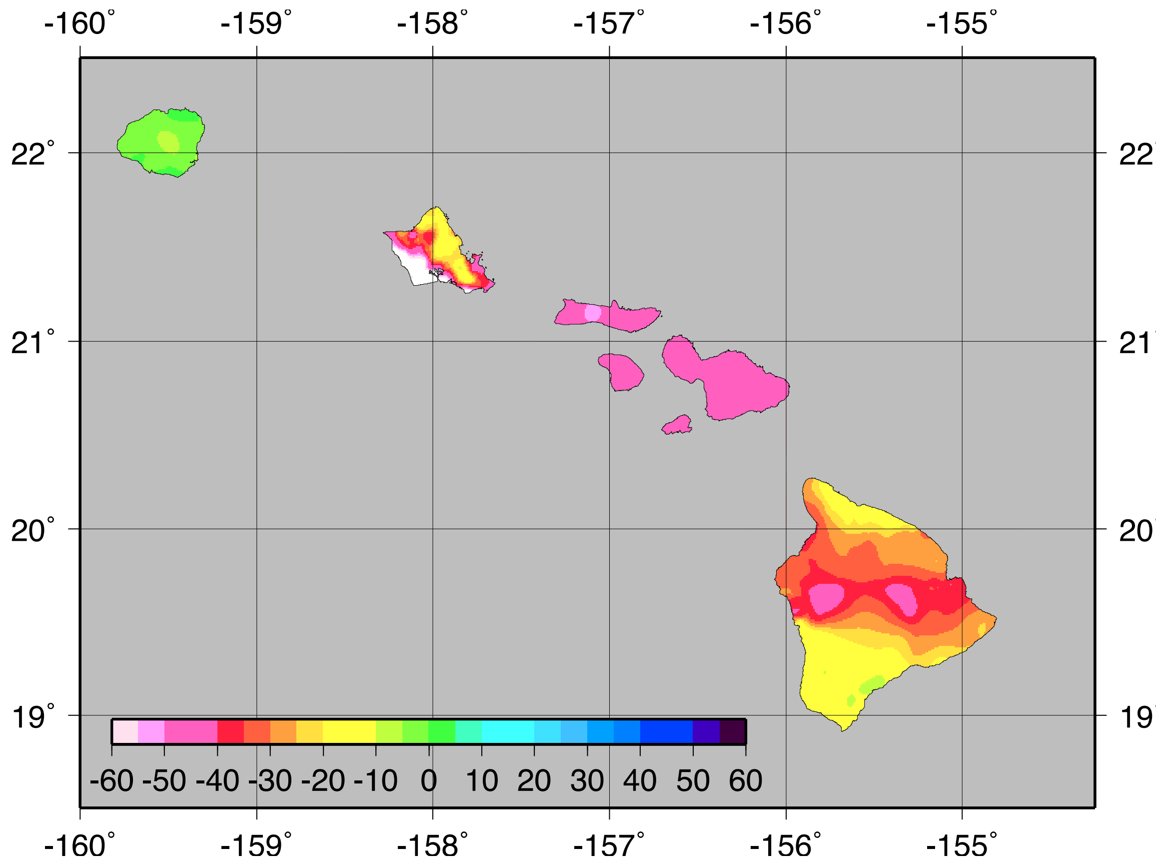

Figure 8: Same as in Figure 7, but for the dry season in the CMIP5 RCP8.5 ensemble median scenario late 21st century (2071-2099 average). Note that the linear regression model estimates very large (negative) anomalies for leeward parts of O'ahu, Maui, Big Island. In general, our confidence in the magnitude of the estimated extreme anomalies are low for the estimates obtained with our linear statistical downscaling for the ensemble median in the more severe RCP 8.5 scenario by end of the century. However, qualitatively the patterns of the rainfall changes remain stable (see Figure 5-8).

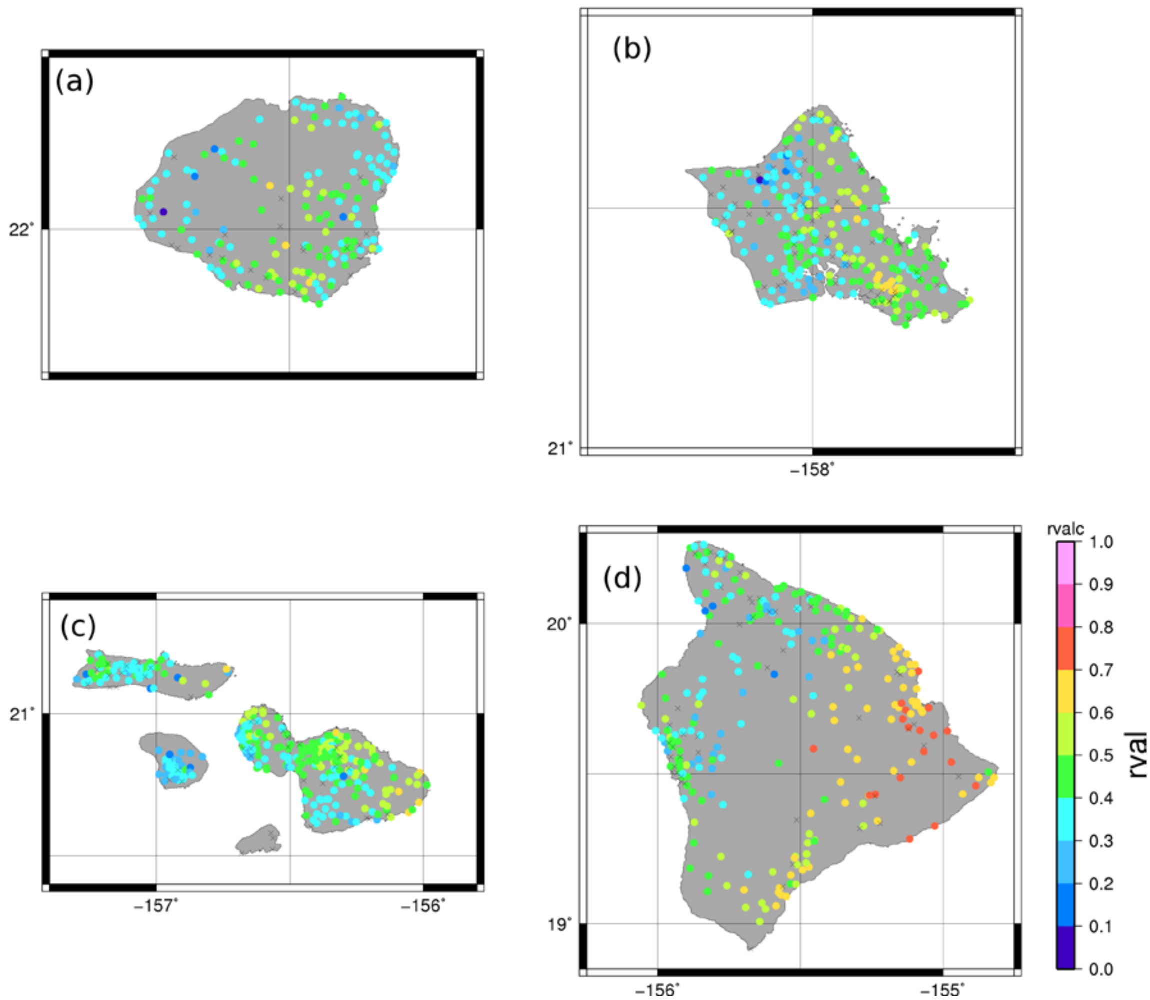

Figure 9: Cross-validation correlation coefficients for the wet season at the individual stations.

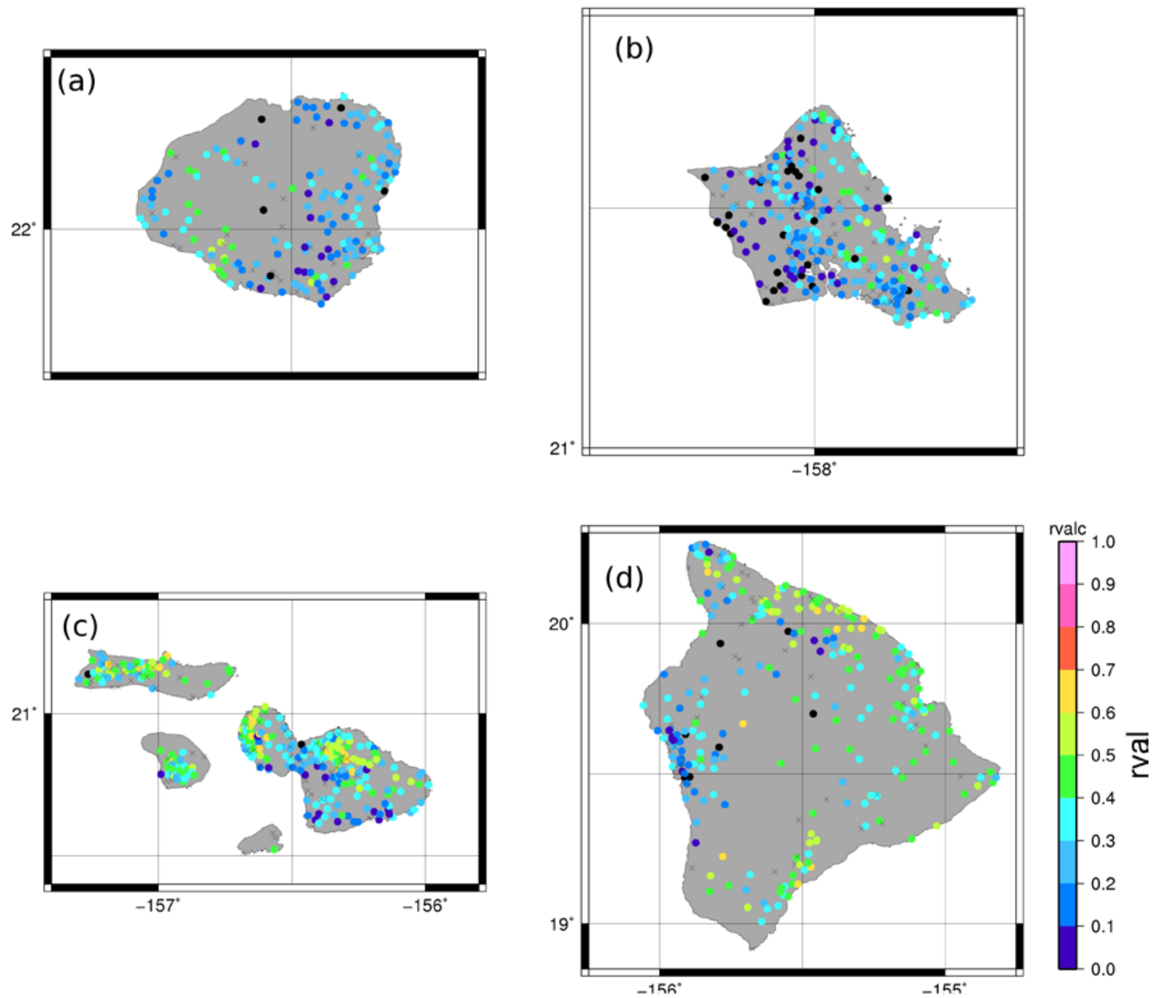

Figure 10: Cross-validation correlation coefficients for the dry season at the individual stations.

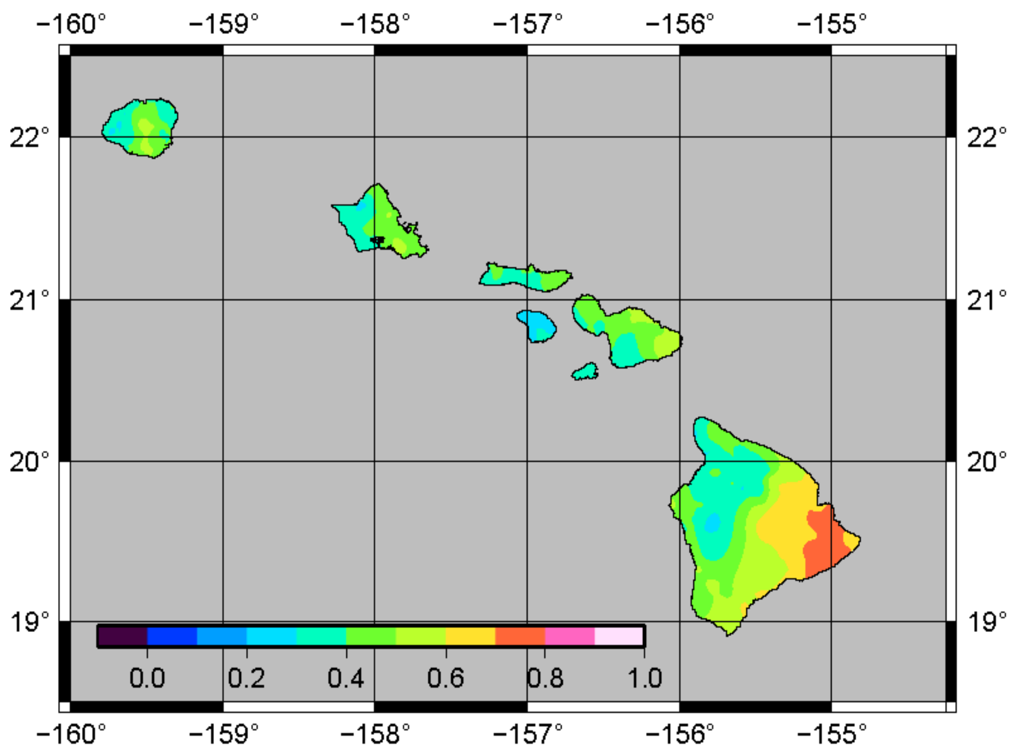

Figure 11: Interpolated correlation skill estimated with Monte Carlo cross-validation methods for the wet season statistical downscaling model. Positive correlations indicate a statistically significant skill for year-to-year fluctuations in the rainfall anomalies 1978-2007. Colors in the light green to orange range (0.5-0.8) are areas with the most robust downscaling results. In general, higher skills are obtained in areas with high precipitation amounts (compare Rainfall Atlas of Hawai'i).

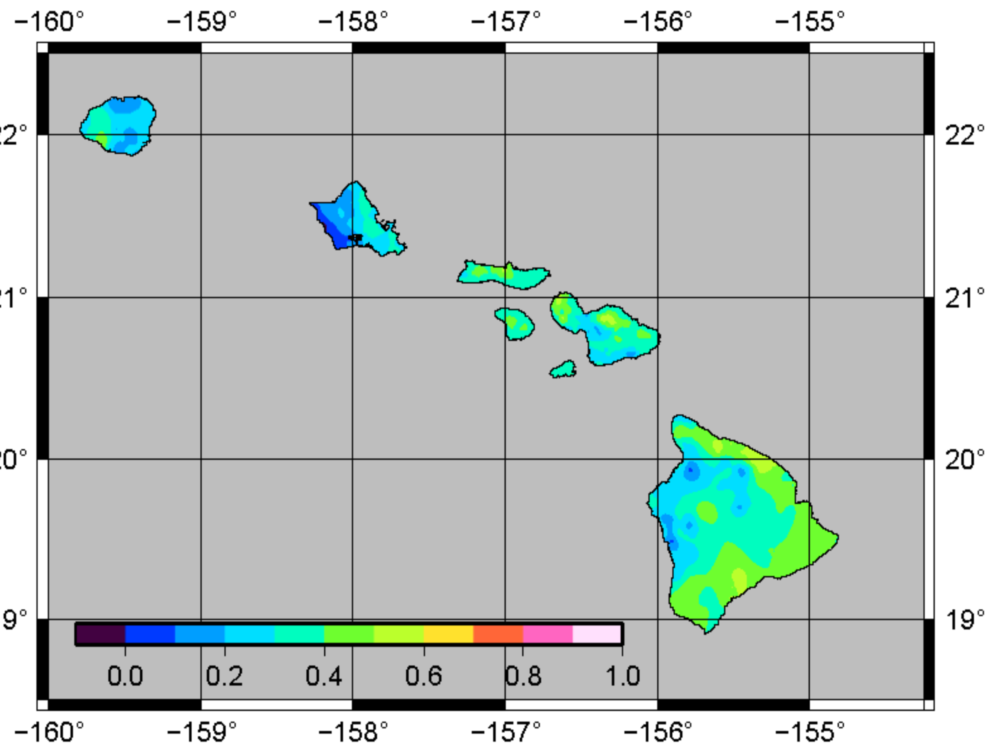

Figure 12: Same as Figure 11, but for the dry season. Note that the overall skill of the statistical downscaling is much lower than in the wet season. Leeward sites of O'ahu indicate no significant skill for individual year-to-year rainfall fluctuations in the dry season. Low correlations between the observed and downscaled rainfall anomalies are found over Kaua'i, O'ahu, dry regions on Maui and the Big Island, in general. Our statistical downscaling provides best skills on the windward sites of Molokai, Maui Big Island. We note that the weaker skill for statistical downscaling during the dry season is in itself consistent with our understanding of how large-scale circulation has a weaker control on the few isolated rainfall events during the generally dry summers.

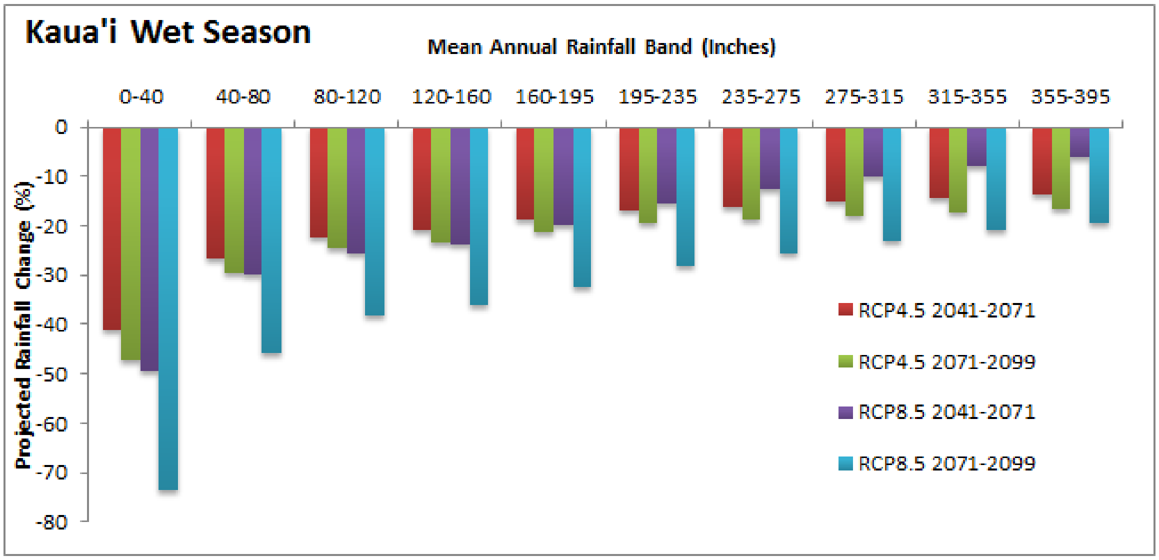

Figure 13: Summary statistics for the Island Kaua'i: Downscaled rainfall anomalies for the wet season averaged over different mean rainfall bands. Rain bands are regions where the climatological rainfall amounts in the season are between the upper and lower bounds expressed in this chart on the top (0-40, 40-80, … 355-395 inches). These regions can be found on the Rainfall Atlas of Hawai'i (http://rainfall.geography.hawaii.edu/). The colored bars indicate averages for the expected changes in the RCP 4.5 and RCP 8.5 scenarios in the mid and late 21st century. The changes are here expressed as projected percentage changes from current climatology.

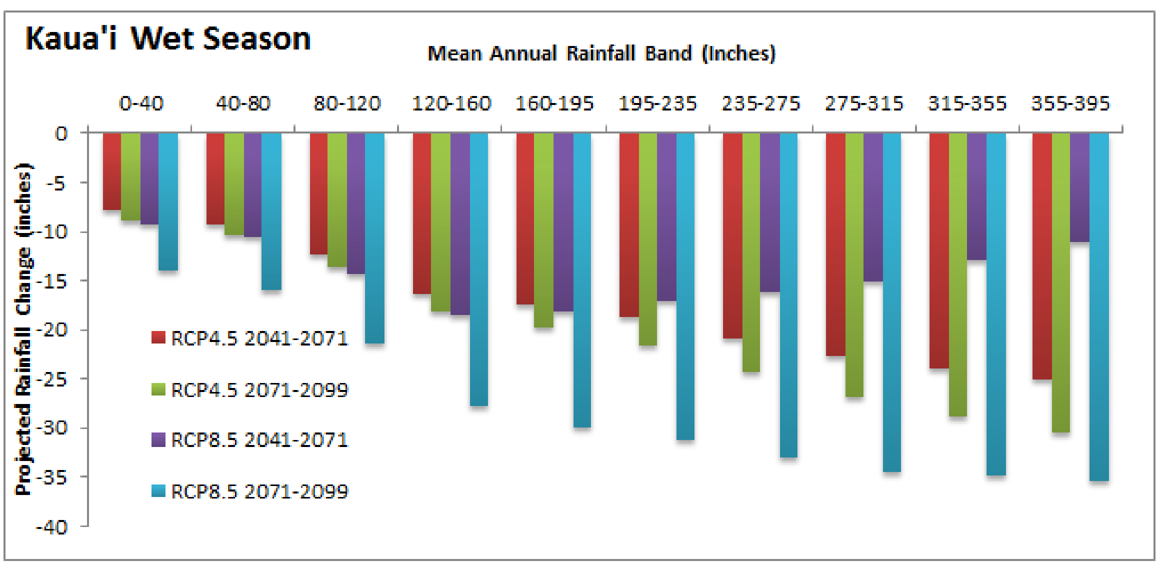

Figure 14: Summary statistics for the Island Kaua'i as in Figure 13 but the rainfall changes expressed in inches.

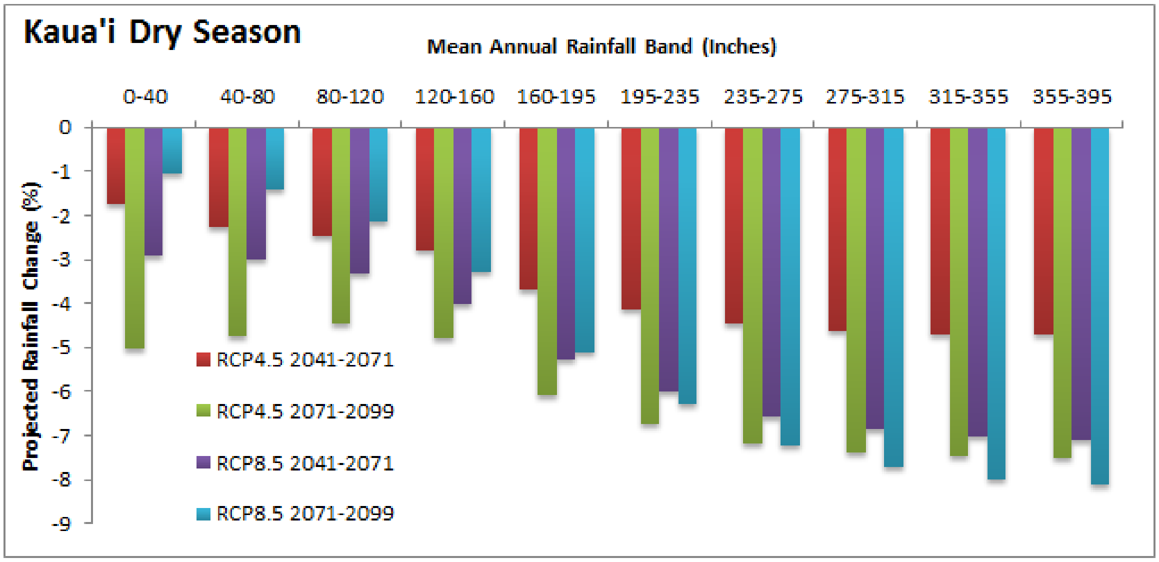

Figure 15: Summary statistics for the Island Kaua'i as in Figure 13 but for the dry season in relative changes (percent).

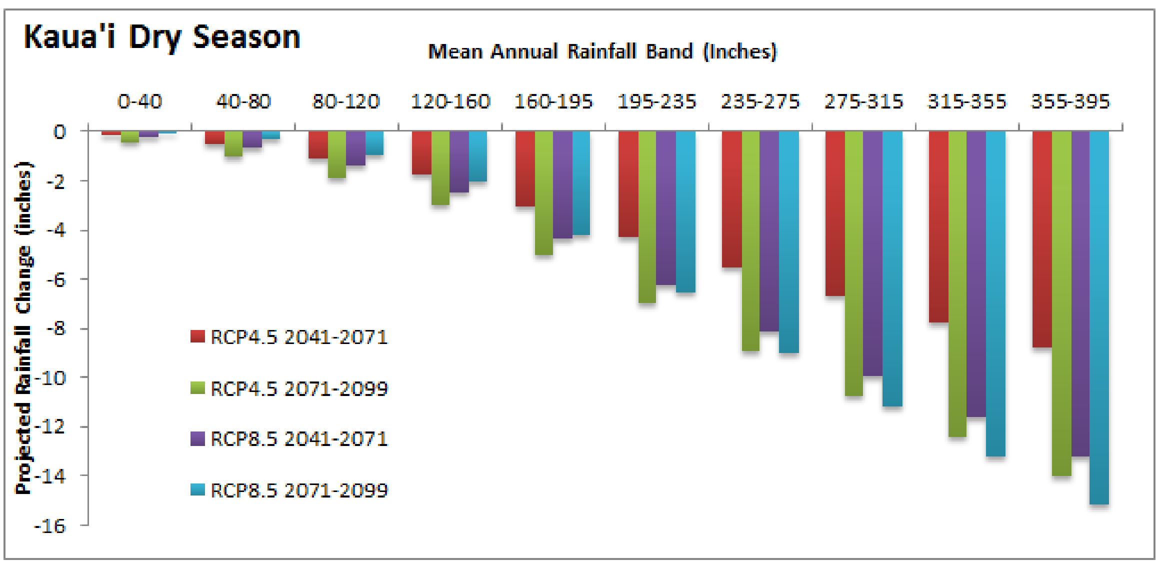

Figure 16: Summary statistics for the Island Kaua'i as Figure 15 but changes expressed in inches.

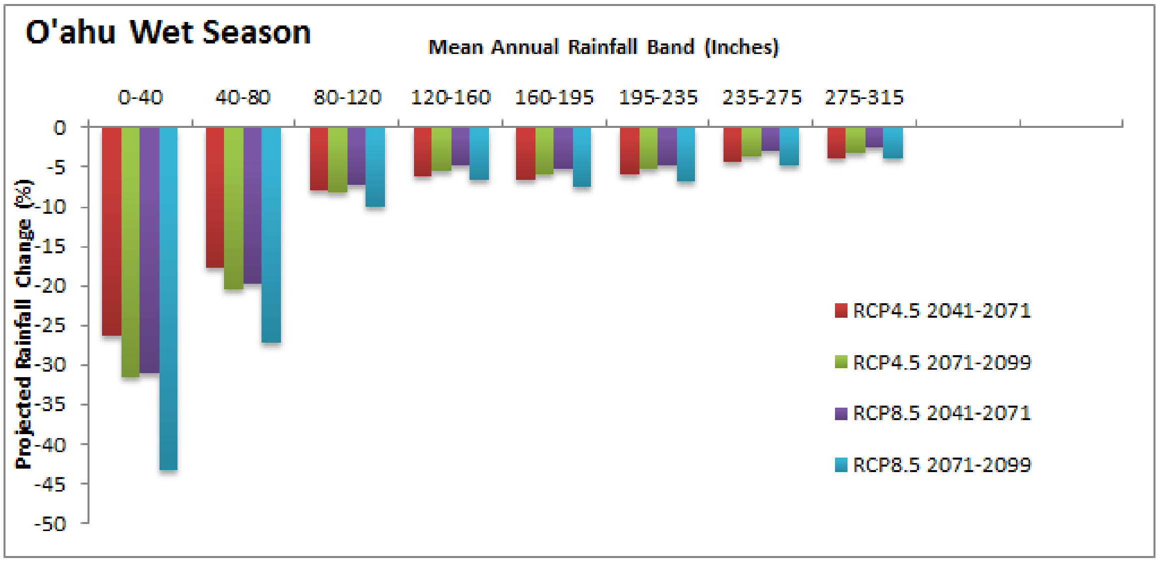

Figure 17: Summary statistics for the Island O'ahu: Wet season changes in different rain bands in percent. See Figure 13 for details.

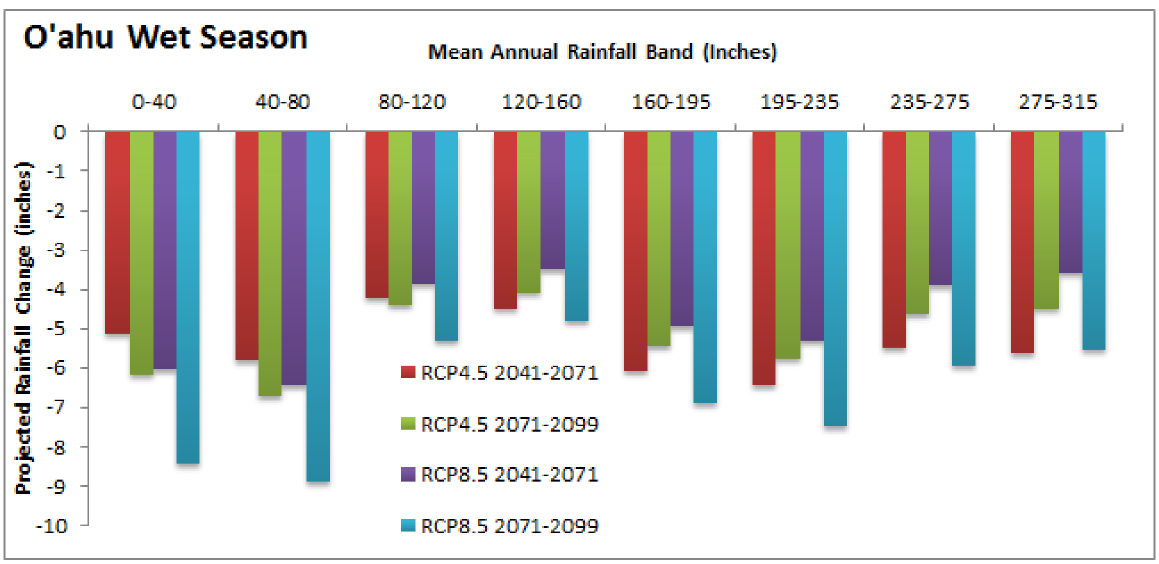

Figure 18: Summary statistics for the Island O'ahu: Wet season changes in different rain bands in inches.

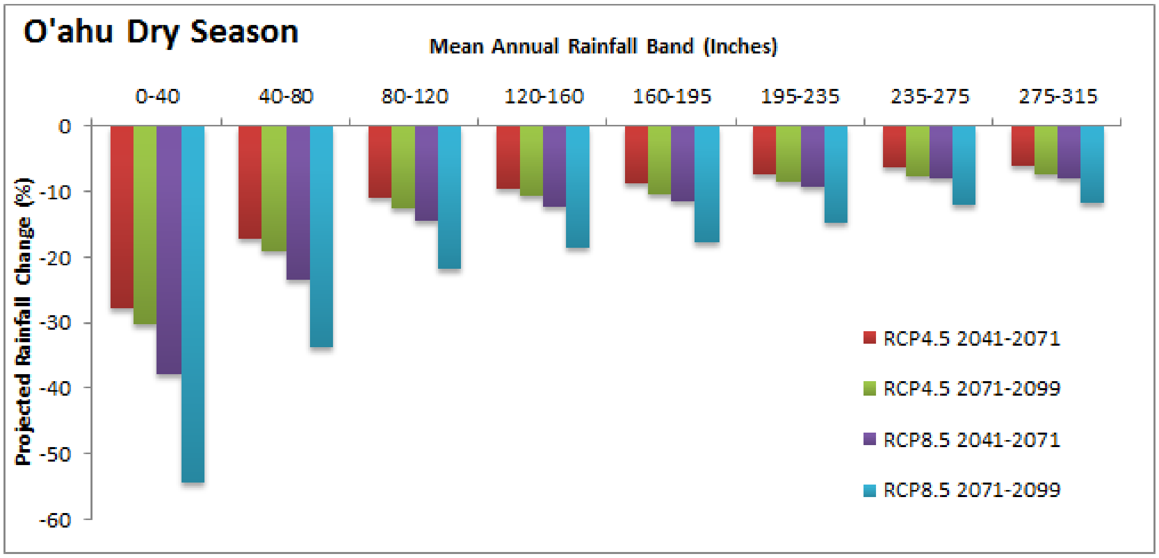

Figure 19: Summary statistics for the Island O'ahu: Dry season changes in different rain bands in percent.

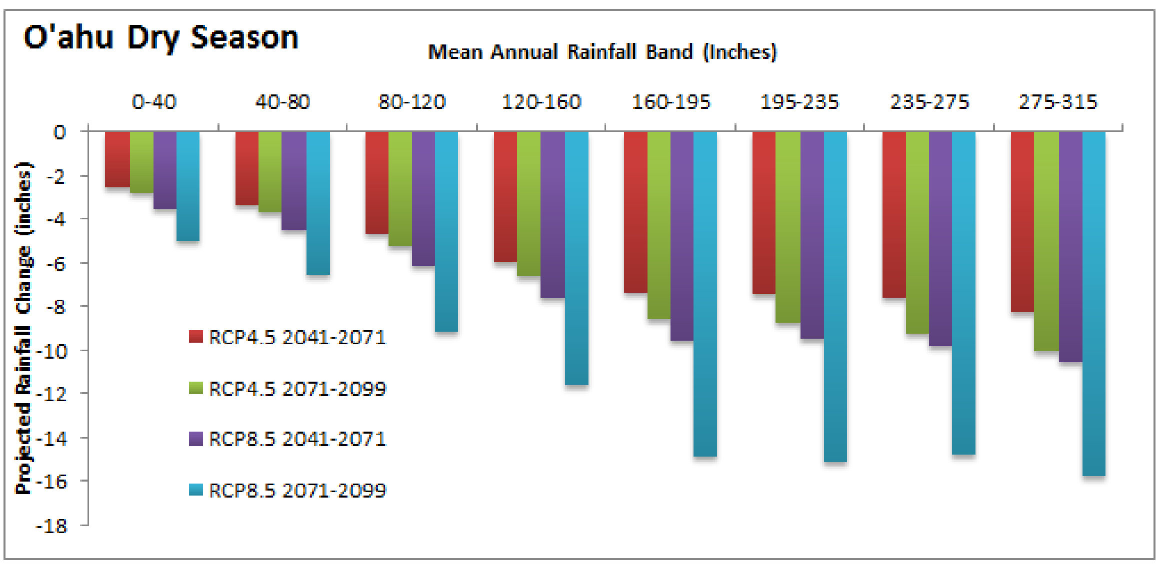

Figure 20: Summary statistics for the Island O'ahu: Dry season changes in different rain bands in inches.

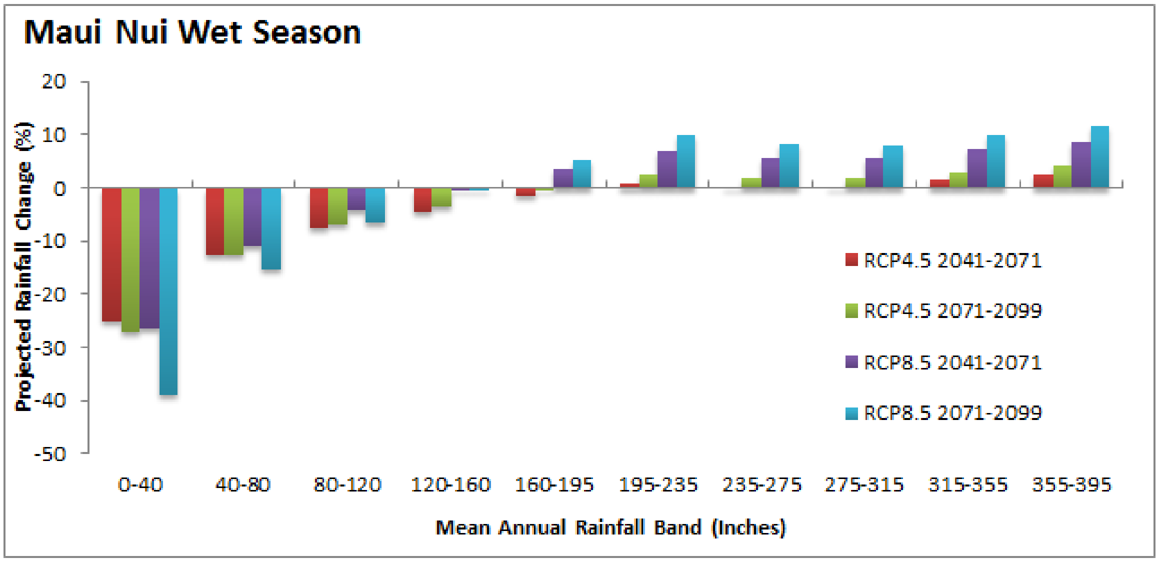

Figure 21: Summary statistics for Maui Nui: Wet season changes in different rain bands in percent.

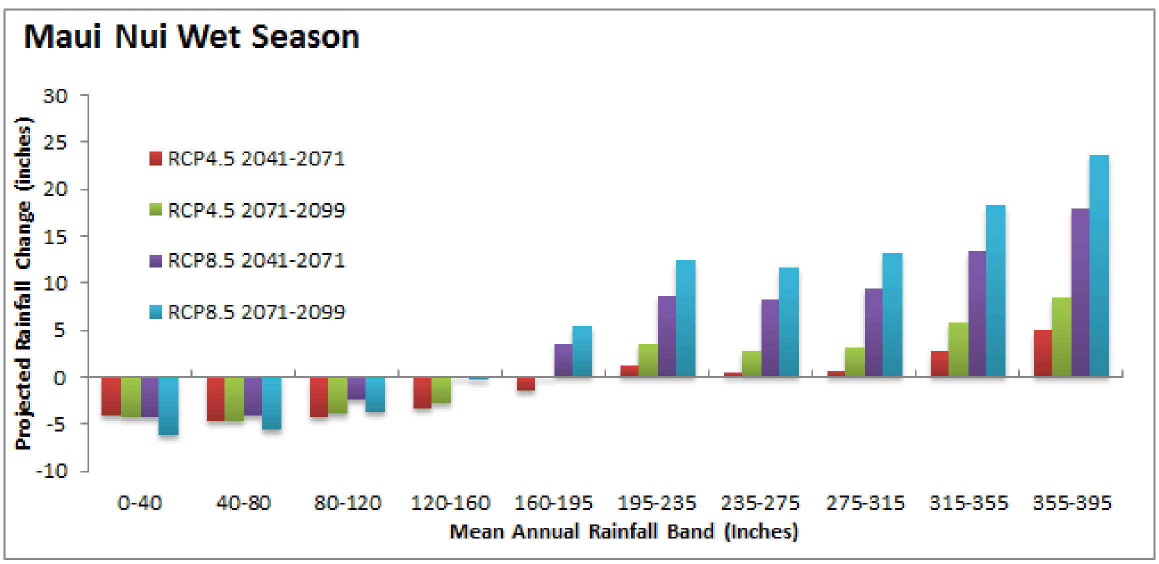

Figure 22: Summary statistics for the Maui Nui: Wet season changes in different rain bands in inches.

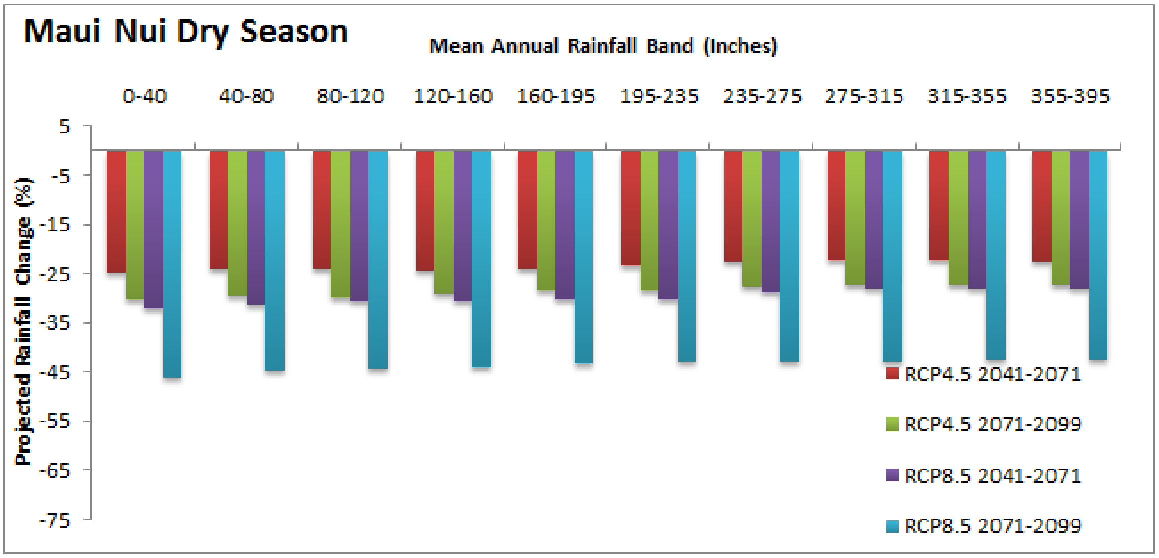

Figure 23: Summary statistics for the Maui Nui: Dry season changes in different rain bands in percent.

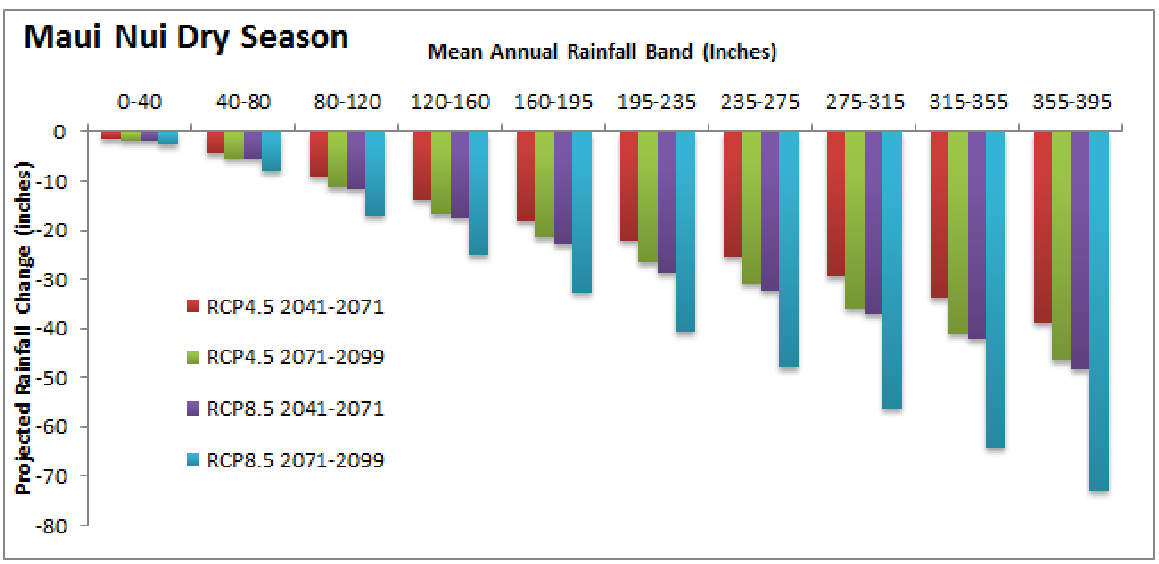

Figure 24: Summary statistics for the Maui Nui: Dry season changes in different rain bands in inches.

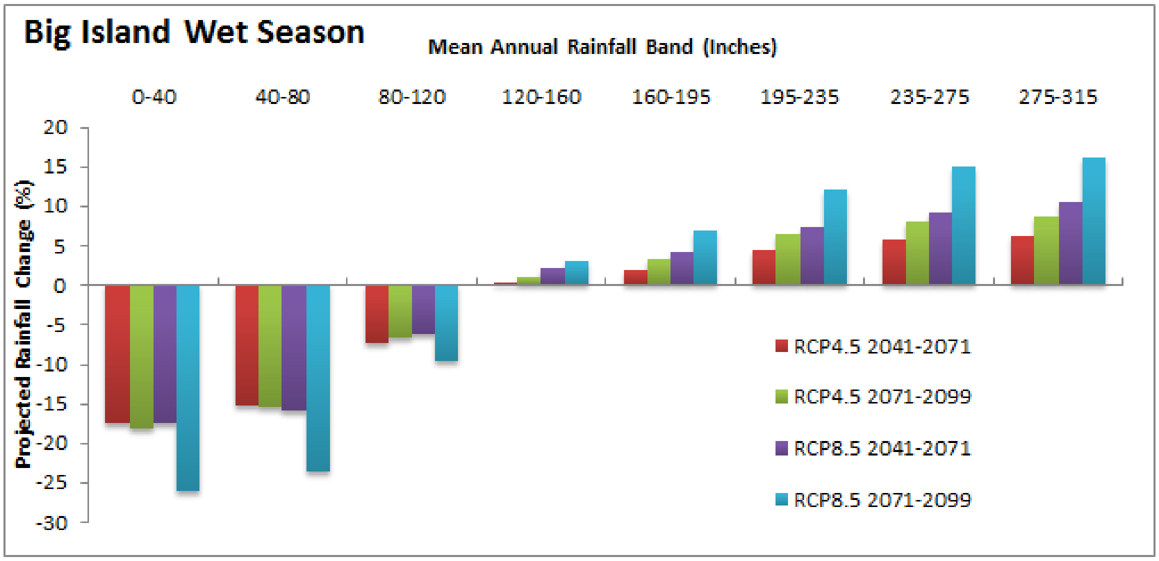

Figure 25: Summary statistics for the Island Hawai'i: Wet season changes in different rain bands in percent.

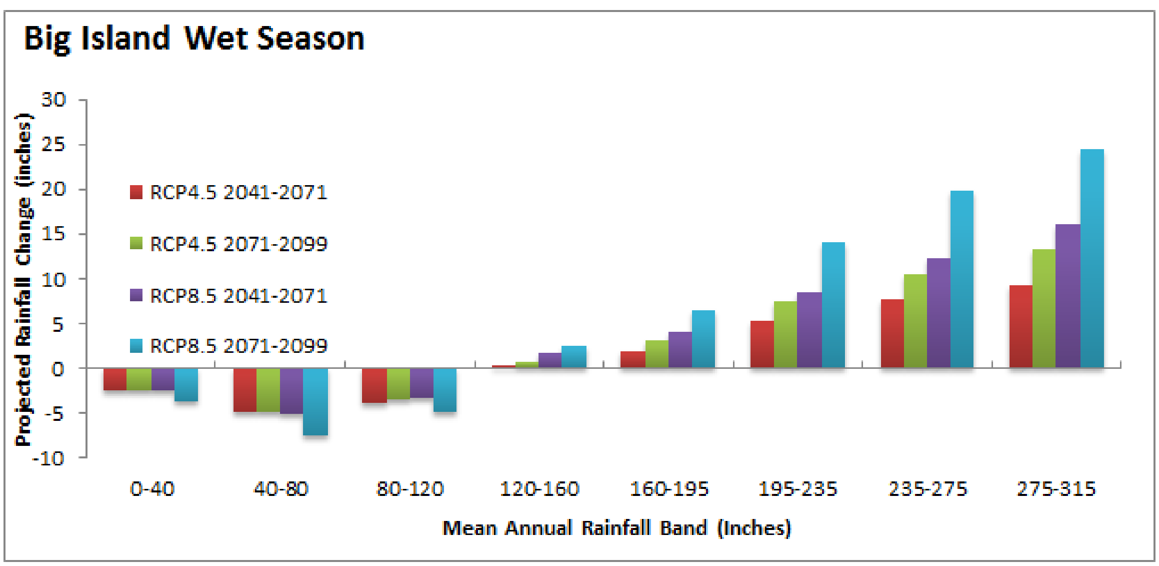

Figure 26: Summary statistics for the Island Hawai'i: Wet season changes in different rain bands in inches.

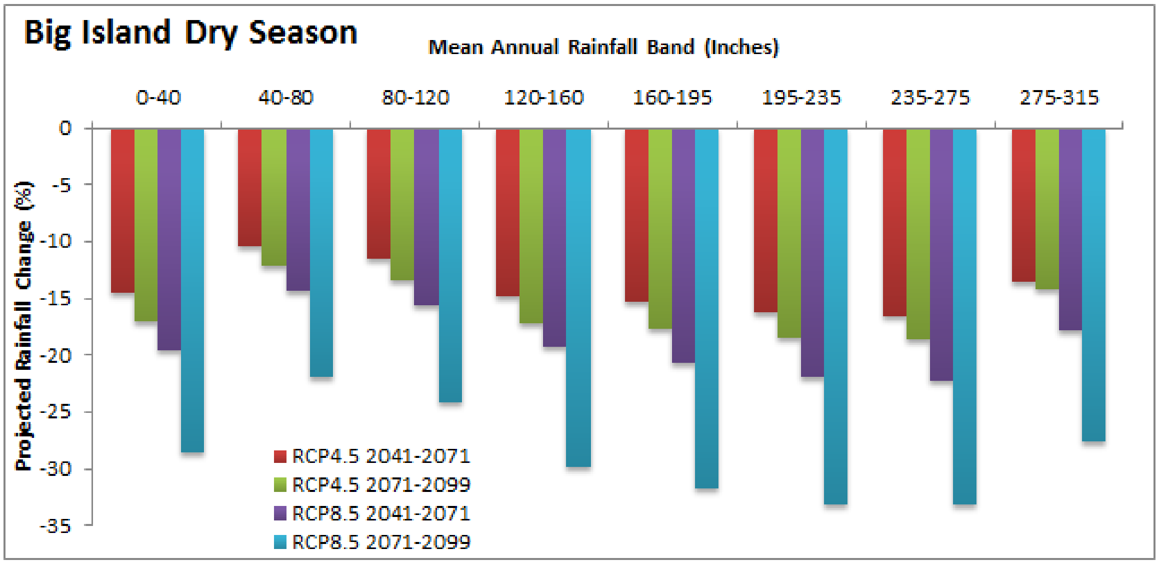

Figure 27: Summary statistics for the Island Hawai'i: Dry season changes in different rain bands in percent.

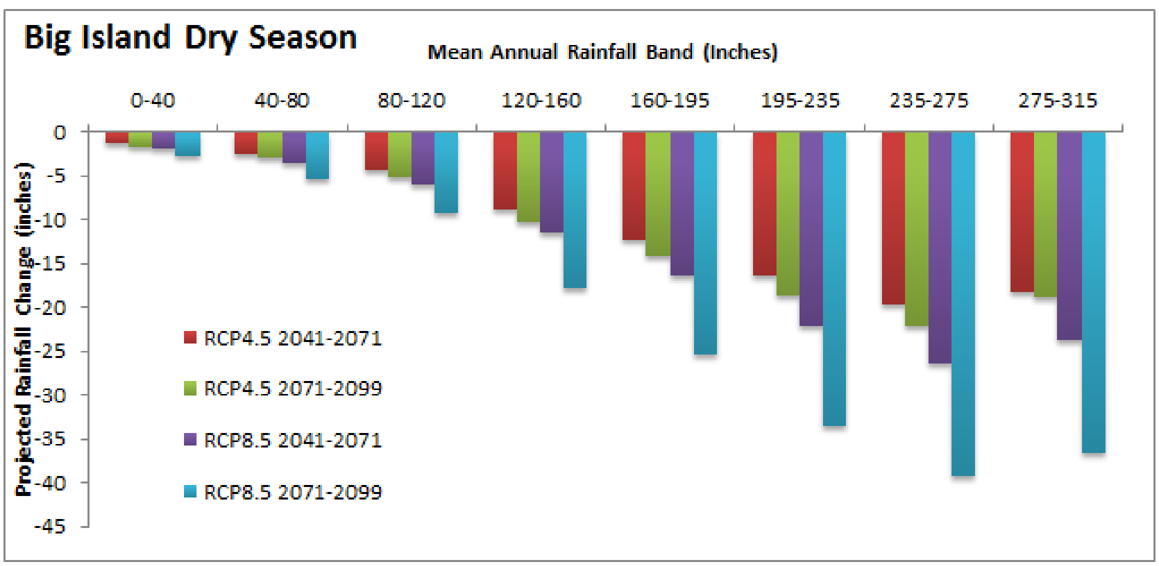

Figure 28: Summary statistics for the Island Hawai'i: Dry season changes in different rain bands in inches.

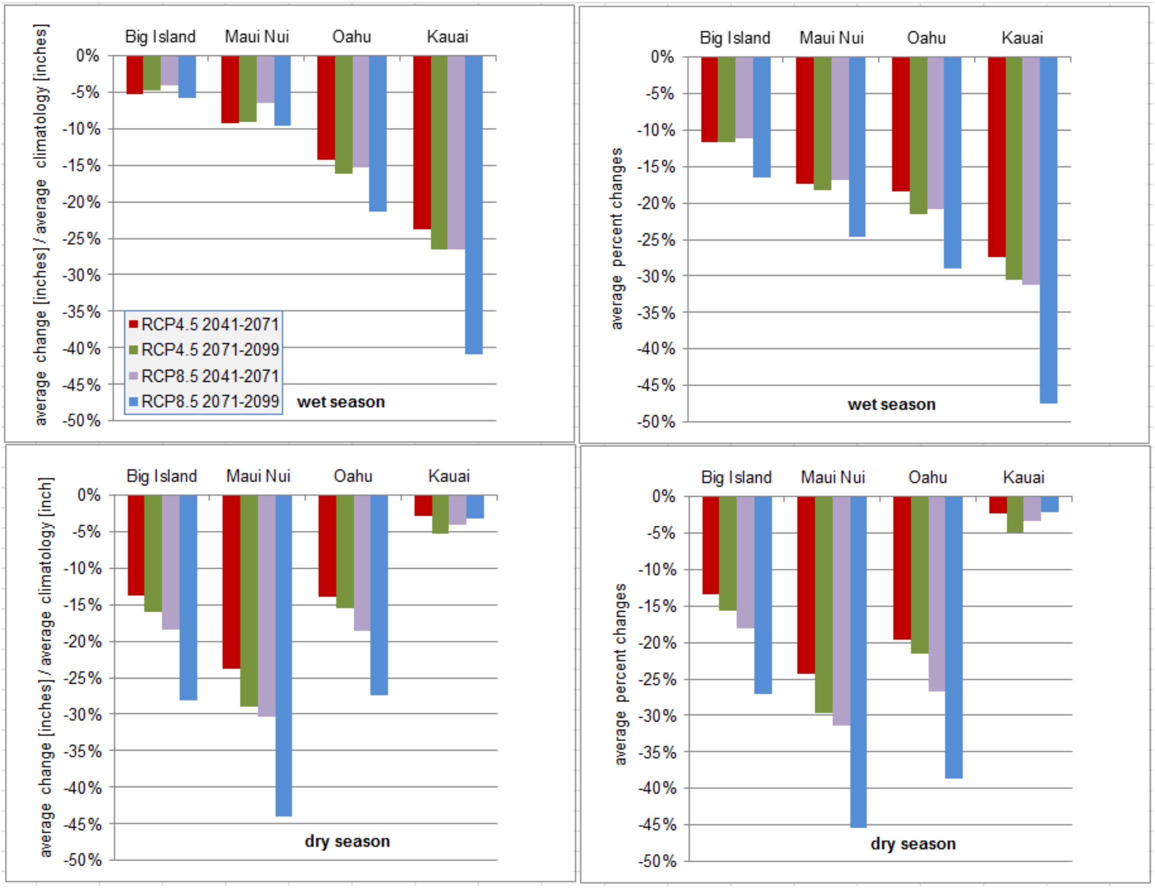

Figure 29: Summary statistics of the relative rainfall changes averaged over the four different island groups. Top left, the average change per island group when translating the downscaled rainfall anomalies first into units of inches and then averaged over the islands and divided by the present-day average rainfall amount in inches. Top right, the island-average rainfall change when averaging the percentage rainfall anomalies (shown in Figs. 1-8) directly. Bottom figures show the results for the dry season. Different scenarios are shown in groups of colored bars (see legend) for each of the four island groups.

C. Products

C.1 Data files

Data sets with statistical downscaling scenarios are available for the following island groups: Hawai'i (BI), Maui Nui (MA), O'ahu (OA), and Kaua'i (KA).Two scenarios from the CMIP 5 database were analyzed: a moderate warming scenario RCP 4.5 and a more severe warming scenario RCP 8.5. Wet and dry seasons were analyzed and downscaled separately: November-April (wet season), and May-Oct (dry season). Two time horizons were chosen: a mid-century and late-century scenario, 2041-2071 and 2071-2099, respectively. The maps shown in Figs. 1-8 are based on the data files having the file name convention:

- **Interpolated precipitation anomaly map data**

cmip?_rcp??_ensemble_precip_ano_stat_???_??_????-????_kc.nc

Where the '?' are placeholders to distinguish separate files representing separate scenarios. Here we only present results based on CMIP5 models, so all files start with 'cmip5'. For example:

cmip5_rcp45_ensemble_precip_ano_stat_wet_OA_2041-2071_kc.nc

cmip5_rcp45_ensemble_precip_ano_stat_wet_OA_2041-2071_kc.csv

This file is the CMIP5 ensemble median RCP4.5 scenario for the wet season, for the Island of Oahu, averaged over the year 2041-2071. The ending ".nc" indicated NETCDF data format (for users of climate data analysis software). The ending ".csv" indicates the corresponding plain-text (ASCII) spreadsheet tables (CSV-format) with longitudes and latitudes in the two columns labelled 'lon' and 'lat', respectively. The units are in degrees east and degrees north. The column 'pr' is the precipitation anomaly in units of % with respect to the climatological means. The last column labelled 'err' is the error variance (the square root gives an estimate for the standard deviation in the same unit as the precipitation anomalies) estimated in the kriging-process (the spatial interpolation error). Note that the interpolation onto the gridded field from the station data locations was done without applying a land-sea mask. The data values are also extrapolated over open oceans. The table below summarizes all combinations. In total there are 32 files.

Island	Scenario	Season	Year 20xx-20xx	Format
BI,OA,MA,KA	RCP 4.5, 8.5	Wet, dry	41-71, 71-99	CSV, NETCDF

Table 1 Summary of the produced downscaling scenarios. These data are stored in the directory: PRODUCTS/DATA/SCENARIOS.

- **Monte Carlo Cross Validation**

The results from the Monte-Carlo Cross Validation shown as interpolated maps are provided in form of NETCDF files and CSV spreadsheet tables. They are located in the directory PRODUCTS/DATA/SDMODEL

mc_val_???_??_kc.csv
mc_val_???_??_kc.nc

e.g. mc_val_dry_BI_kc.nc is the NETCDF version of the interpolated cross-validation results for the dry season on Big Island. The spreadsheet version has the ending ".csv"

We note that we have provided additional data of the statistical downscaling model calibration in subdirectories for each island group and season in
composite_cal_ncepgrid_ndjfma_??
composite_cal_ncepgrid_mjjaso_??

They contain several files with the full information on the statistical model parameters and the corresponding predictor time series:

composite.cal.export.param.ndjfma.1978-2007.csv
pc.cal.csv

In this example, the wet season (ndjfma is the wet season, mjjaso is the dry season), contains the regression parameters and their error estimates in a spreadsheet table with the station location information (Station ID, longitude, latitude, elevation). The other data sets are of secondary importance but kept for future references in the PRODUCTS.
We strongly recommend contacting the PIs before using these any of these data sets.
In particular, the interpolated gridded files (ending with ".kc.csv") still contain uncorrected latitudes in the spreadsheet table by the time of writing this report.
The other two files starting with "composite.val" and "composite_val" and ending on ".csv" contain earlier attempts of cross-validating the statistical downscaling skill.
We recommend the use of these results only with prior consultation of the PIs.

- **Summary statistics for different rain bands**

Summary statistics shown in figures xx-xx are based on interpolated versions of the data files with the same 250m resolution of the Rainfall Atlas of Hawai‘i. The summary statistics are available in an EXCEL spreadsheet:

PRODUCTS/DATA/SCENARIOS/SummaryStats_MAP_Bands.xlsx

The average statistics for each of the four island groups (Figure 29) is given in the spreadsheet file SummaryIslandStats.xlsx

C.2 Figure Files

We provide the figure of the interpolated maps (Figures 1-8) and the summary statistics figures in the directory PRODUCTS/FIGURES/. The interpolated maps are orginally created in EPS format, which we converted into PDF format.
The summary statistics are delivered here a PNG files. They are also contained in the Spreadsheet file itself and can be copied or exported from the EXCEL file if other resolutions or formats are preferred by the user.

- **Interpolated rainfall anomaly maps**

map_cmip5_rcp??_ensemble_precip_ano_stat_???_HI_20??-20??_median_kc.pdf

These maps were produced with the Generic Mapping Tools (GMT V4.3.1) using a Mercator projection ("psbasemap –R-160/-154.25/18/5/22.5 –JM16c") .

Again, RCP 4.5 and 8.5 scenarios season wet/dry and time horizons 2041-2071, 2071-2099 are indicated by the placeholders '?'.

- **Summary statistics**

The summary statistics shown in Figures 13-28 are in PRODUCTS/FIGURES/

SummaryStats_MAP_Bands_??_???_perc.png
SummaryStat_MAP_Bands_??_???_in.png

For example: SummaryStat_MAP_Bands_BI_wet_in.png is the rainfall change summary for Big Island in the wet season expressed in units of inches.
SummaryStat_MAP_Bands_BI_wet_perc.png is the same expressed in percent changes.

The summary statistics in Figure 29 are in the file SummaryIslandStats.xlsx

- **Monte Carlo Cross Validation**

The Monte Carlo cross validation statistics figures (11,12) are:

map_mc_val_wet_HI_1978-2007.pdf
map_mc_val_dry_HI_1978-2007.pdf

(We also included the EPS- versions)

Figures with station values plotted on the maps (Figures 9,10)

map_2x2_stat_wet_rval.png
map_2x2_stat_dry_rval.png

We also included the corresponding maps for the calibration statistics, which we have not shown in this report, because the cross validation skill provides a more conservative correlation value.

D. References

[1] Giambelluca, T.W., Q. Chen, A.G. Frazier, J.P. Price, Y.-L. Chen, P.-S. Chu, J.K. Eischeid, and D.M. Delparte, 2013: Online Rainfall Atlas of Hawai‘i. Bull. Amer. Meteor. Soc., 94,313-316, doi: 10.1175/BAMS-D-11-00228.1

[2] Elison Timm, O., H. F. Diaz, T. W. Giambelluca, and M. Takahashi (2011), Projection of changes in the frequency of heavy rain events over Hawai‘i based on leading Pacific climate modes, , J. Geophys. Res.: Atmos., 116(D4), 1–12, doi:10.1029/2010JD014923

[3] Elison Timm, O., M.Takahashi, T. W. Giambelluca and H. F. Diaz, 2013: On the relation between large-scale circulation pattern and heavy rain events over the Hawaiian Islands: Recent trends and future changes, J. Geophys. Res.: Atmos., 118, 1–13, doi:10.1002/jgrd.50314.